Supporting Information

Decoupling Light- and Oxygen-Induced Degradation Mechanisms of Sn-Pb Perovskite in All Perovskite Tandem Solar Cells

Supporting Information

Yang Bai[1,2†], Ruijia Tian[1†], Kexuan Sun[1†], Chang Liu[1]*, Xiting Lang[1], Ming Yang[1], Yuanyuan Meng[1], Chuanxiao Xiao[1], Yaohua Wang[1], Xiaoyi Lu[1], Jingnan Wang[1], Haibin Pan[1], Zhenhua Song[1], Shujing Zhou[1], and Ziyi Ge[1,2*]

[1]Zhejiang Provincial Engineering Research Center of Energy Optoelectronic Materials and Devices, Ningbo Institute of Materials Technology & Engineering, Chinese Academy of Sciences, Ningbo 315201, China

[2] Center of Materials Science and Optoelectronics Engineering, University of Chinese Academy of Sciences, Beijing 100049, China

† Yang Bai, Ruijia Tian and Kexuan Sun contributed equally to this work.
*Corresponding authors: E-mail: liuchang1@nimte.ac.cn; geziyi@nimte.ac.cn

Experimental method

Materials

All the materials were used as received without purification. Formamidinium iodide (FAI, 99.99%), methylammonium chloride (MACl 99.99%), PbI_2 (99.9%), lead (II) chloride ($PbCl_2$ 99.9%), SnI_2 (99.9%), Nickel oxide (NiO_x) and patterned ITO substrates were purchased from Advanced Election Technology CO., Ltd.. Methylammonium iodide (MAI), cesium iodide (CsI), lead bromide ($PbBr_2$), and ethanediamine dihydroiodide $(EDAI)_2$ were supplied from Xi'an Polymer Light Technology Corporation. Isopropanol (IPA, 99.9%), chlorobenzene (CB, 99.9%), diethyl ether (DE), N,N-dimethyl formamide (DMF, 99.8%), and dimethyl sulfoxide (DMSO, 99.7%) were obtained from Beijing J&K Scientific Ltd.. PEHCl-OC (97%), PEHCl-F (97%), PEHCl-CN (97%) and MBI (99%) were procured from Aladdin. Tin(II) fluorine (SnF_2,99%) and ammonium thiocyanate (NH_4SCN, 99.9%) and lead(II) thiocyanate ($Pb(SCN)_2$, 99.9%) were purchased from Sigma-Aldrich. PEDOT: PSS (CLEVIOS P VP AI 4083) was purchased from Heraeus.

NBG $FA_{0.6}MA_{0.3}Cs_{0.1}Pb_{0.5}Sn_{0.5}I_3$ perovskite solution Preparation

Dissolve 414.91 mg PbI_2, 335.27 mg SnI_2, 185.73 mg FAI, 85.84 mg MAI, 46.77 mg CsI, 14.10 mg SnF_2 and 2.57 mg NH_4SCN in 1 mL DMF and DMSO (DMF: DMSO = 3:1, v/v) mixed solution to prepare (1.8 M) perovskite precursors. Finally, the solution was filtered with a 0.22 μm polytetrafluoroethylene (PTFE) membrane before preparing the perovskite film.

WBG $FA_{0.8}Cs_{0.2}PbI_{1.8}Br_{1.2}$ perovskite solution Preparation

Dissolve 212.06 mg PbI_2, 271.58 mg $PbBr_2$, 165.1 mg FAI, 6.67 mg $PbCl_2$, 62.4 mg CsI, 1.62 mg MACl and 4.8mg $Pb(SCN)_2$ in 1 mL DMF and DMSO (DMF: DMSO = 4:1, v/v) mixed solution to prepare of (1.2 M) perovskite precursors.

NBG Sn-Pb perovskite solar cell fabrication

The patterned ITO substrates were firstly ultrasonic cleaned with detergent, deionized water, acetone, and isopropanol for 30 mins in sequence, then dried by N_2 gas and treated with plasma for 5 mins. Subsequently, the prepared ITO substrates were spin-coated with the PEDOT: PSS solution for 30 s at 4000 rpm, then annealed at 150 °C for 15 mins in the air. After that, the film was transferred to the N_2 atmosphere glovebox for further spin-coating. The prepared NBG precursor solution was spin-coated by a two-step process: 1000 rpm for 10 s followed by 4000 rpm for 30 s, and the antisolvent (CB) was dripped at 30 s, and then the films were annealed at 1000 ℃ for 10 min in the glovebox. Next, the $EDAI_2$ (in IPA with a concentration of 1.0 mg ml^{-1}) layer precursor solution was spin-coated at 4000 rpm for 20 s then annealed at 100 ℃ for 1 min. Then, 25 nm of C_{60}, 6 nm of BCP, and 100 nm of Ag were deposited in sequence via thermal evaporation

All-perovskite tandem solar cell fabrication

NiO_x nanocrystal (10 mg ml^{-1} in H_2O) layers were first spin-coated on ITO

substrates at 1500 rpm for 30 s and annealed at 150 °C for 30 min in air. After cooling, the substrates were immediately transferred to the N_2-filled glovebox. In the following, the self-assembled monolayers of Me-4PACz (0.3 mg ml^{-1} in ethanol) were spin-coated on the ITO substrates at 3000 rpm for 30 s, and the substrates were heated at 100 °C for 10 min. The WBG perovskite films were deposited with a two-step spin-coating procedure: 5000 rpm for 2s and 4000 rpm for 60 s DE was dropped onto the spinning substrate during the second spin-coating step at 25s. Then, the substrates were then transferred onto a hotplate and heated at 100 °C for 10 min. After cooling down to room temperature, the substrates were transferred to the evaporation system and a 25 nm C_{60} film was subsequently deposited on. ALD SnO_2 layers with a thickness of 20 nm were deposited on the WBG perovskite films, after which 1.0 nm of Au was deposited via thermal evaporation. PEDOT: PSS layers were spin-coated on top of the front cells at 4000 rpm for 30 s and annealed in air at 120 °C for 20 min. The substrates were then transferred to an N_2-filled glovebox for the fabrication of NBG films. The NBG films were deposited and treated as described above.

Film and device characterization

The Newport oriel sol3A 450 W solar simulator was used to test the current density versus voltage (J–V) curves and stabilized power output (SPO) and steady-state current density curves under AM 1.5G, measure characterize the conductivity and the space-charge-limited current analysis under dark condition. A J-V scan was performed on the Sn-Pb perovskite solar cell with a scan rate of 0.1 V s^{-1} and a delay time of 50 ms. The forward scanning range is -0.1 ~ 1.0 V, and the reverse scanning range is 1.0 ~ -0.1 V. A J-V scan was performed on the all-perovskite tandem solar cell with a scan rate of 0.1 V s^{-1} and a delay time of 50 ms. The forward scan is -0.2 ~ 2.2 V, and the reverse scan is 2.2 ~ -0.2 V. The area of the solar cell under test is 0.0116 cm^2. Place an aperture shading mask in front of the solar cell to ensure that the effective area is 0.06 cm^2. The solar cell quantum efficiency test system (Elli Technology Taiwan) was used to measure the EQE spectra of devices. The Mott-Schottky curves and the impedance spectroscopy (IS) were determined with the Chenhua CHI760E electrochemical workstation. The t-DOSs curves were recorded by the 1240A Impedance Analyzer. EQE measurements were measured by applying external voltage/current sources through the PSCs with a REPS measurement instrument (Enlitech). Operational stability tests of NBG/tandem solar cells were performed at maximum power point (MPP) in N_2 environment under AM1.5 xenon lamp illumination (100 mW cm^{-2}, without UV filter). The Time-of-Flight Secondary Ion Mass Spectrometry (TOF-SIMS) analysis was performed using a dual-beam approach. Primary ion bombardment was carried out using Bismuth (Bi^{3+}) ions at an energy of 30 keV and a current of 45 degrees per nanoampere. Secondary ion detection was facilitated by Cesium (Cs^+) ions at an energy of 1 keV and a current of 80 nanoamps, with the secondary ion beam aligned at 45 degrees to the primary ion path. Additionally, a flood gun was employed to neutralize the charge on the sample surface, ensuring accurate mass resolution and ion yield.

The FTIR spectroscopy was detected by FTIR-8400S (Shimadzu). XPS was measured by Kratos axial super dald. For the calibration of XPS data, the instrument was calibrated using the binding energy positions of Au $4f_{7/2}$, Ag $3d_{5/2}$, and Cu $2p_{3/2}$ spectral peaks, respectively. The calibration error of instrument is G0.10 eV, and the binding energy error during the test is within 0.1 eV. The binding energy of the measured XPS data correction was performed using C 1s spectrum (284.8 eV). Both instrumental calibration and spectra correction ensure the accuracy of data interpretation. For the binding energy calibration of the UPS spectrum, the energy scale of the spectrometer system is linearly calibrated by Au, Ag, and Cu standard materials. The Fermi edge of Au or Ag reference materials is then used to calibrate the kinetic energy scale relative to the Fermi edge of the sample. The photon energy used is 21.22 eV. To avoid unwanted contamination, the samples have been carefully sealed in N_2-fifilled glovebox and been taken out right before the test. SEM images were obtained by scanning electron microscope (verios G4 UC) (Rimono Scientifific Company, USA) at 2 kV. The steady PL spectra were recorded on the Horiba jobin Yvon flfluorolog-3 spectrofluorometer system and PL mapping was measured by HORIBA HR Evolution. TRPL was analyzed by the FLS 980 fluorescence spectrometer equipped with a 532 nm excitation. The KPFM images were captured by Dimension ICON SPM (Dimension Icon, German). Chi 660e electrochemical measurement workstation (Chengdu equipment company, Shanghai, China) was used for SCLC analysis under dark conditions. Depth-resolved GIXRD were characterized using a Rigaku SmartLab fifive-axis X-ray diffractometer at 45 kV and 200 mA, equipped with Cu Ka radiation (l = 1.54050 A˚), parallel beam optics and a secondary graphite monochromator.

Simulation

The DFT calculations in this research are performed using the Vienna ab initio simulation software (VASP). To simulate electron exchange-related interactions, the Perdew–Burke–Ernzerhof (PBE) functional is utilized, and the projection enhanced wave (PAW) approach is used for electron–ion–nucleus interactions. In order to handle van der Waals interactions in perovskites, we employ the Grimme DFT-D3 approach with Becke-Johnson damping. Geometry optimization is carried out with the Γ-centered 2×2×2 Monkhorst−Pack k-point mesh and the 400eV plane wave energy cutoff. The geometric structure is regarded as convergent when the energy difference between all ions is smaller than -10^{-4} eV. After completing the structural optimization calculation, we established a defect model based on the optimized perovskite surface model and adsorbed PEHCl-X or MBI on its surface to simulate the effect of adsorbed organic ions on surface defects.

The electrostatic potential (φ_{max}) calculations were carried out by using the Gaussian 16 program. The Becke three parameters hybrid exchange-correlation functional (B3LYP) level of theory combined with the 6-311+G(d) standard basis set was adopted. The dispersion correction schemes by Grimme (denoted as D3) were used to account for the van der Waals interactions. For the geometry optimization procedure, the structures were optimized until the forces were $< 10^{-5}$

hartree/bohr and the energy change was < 10^{-7} hartree. The convergence criterion for the energy calculation during the self-consistent-field procedure was set for < 10^{-8} hartree.

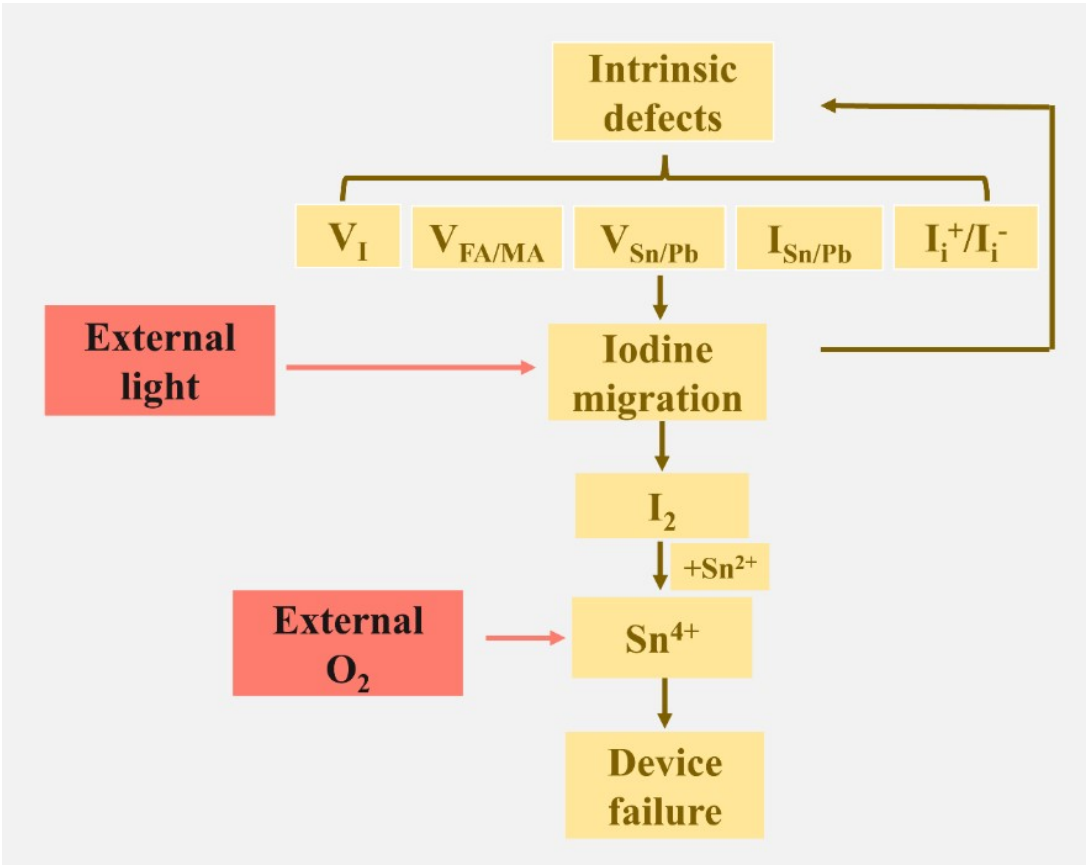

Figure S1. Degradation pathway description of tin-lead perovskite

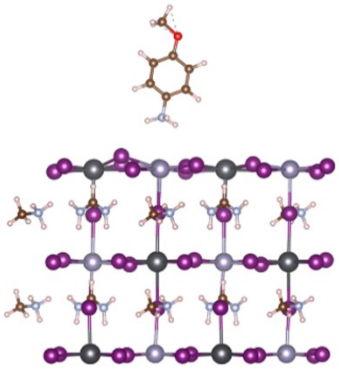

Figure S2. Binding energies of 4-Methoxyaniline hydrochloride (PA^+-OC) on the Sn-Pb perovskite surface.

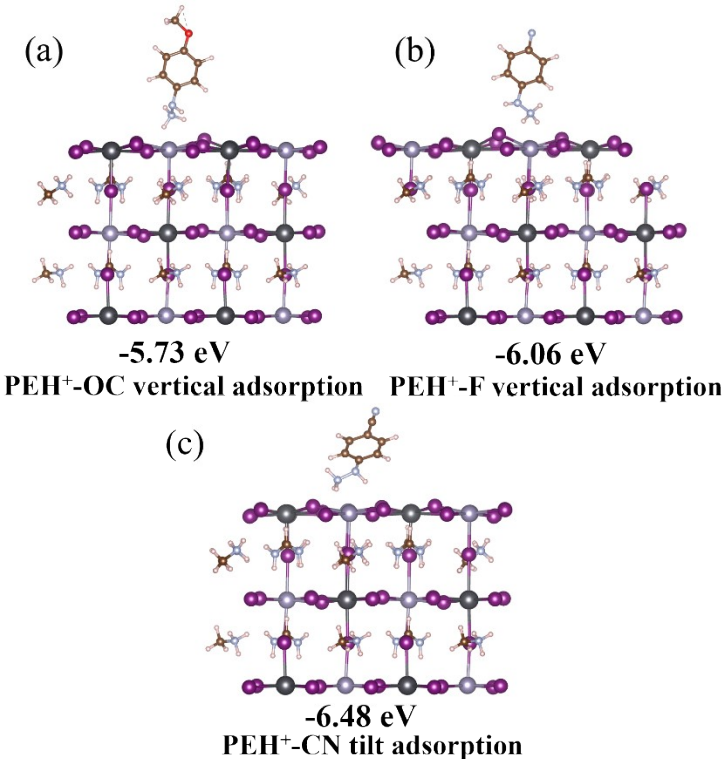

Figure S3. The optimal adsorption configuration and binding energy of (a) PEH$^+$-OC, (b) PEH$^+$-F, and (c) PEH$^+$-CN on the perovskite surface.

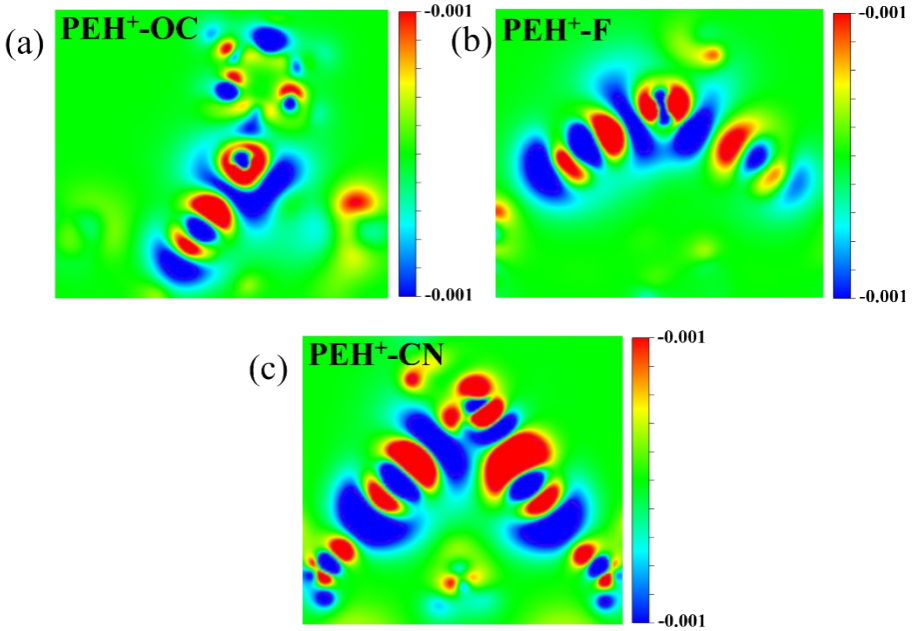

Figure S4. Cross-sectional distribution of charge density of (a) PEH$^+$-OC, (b) PEH$^+$-F, and (c) PEH$^+$-CN after absorption on perovskite. Red represents areas of increased charge, while blue indicates areas of decreased charge.

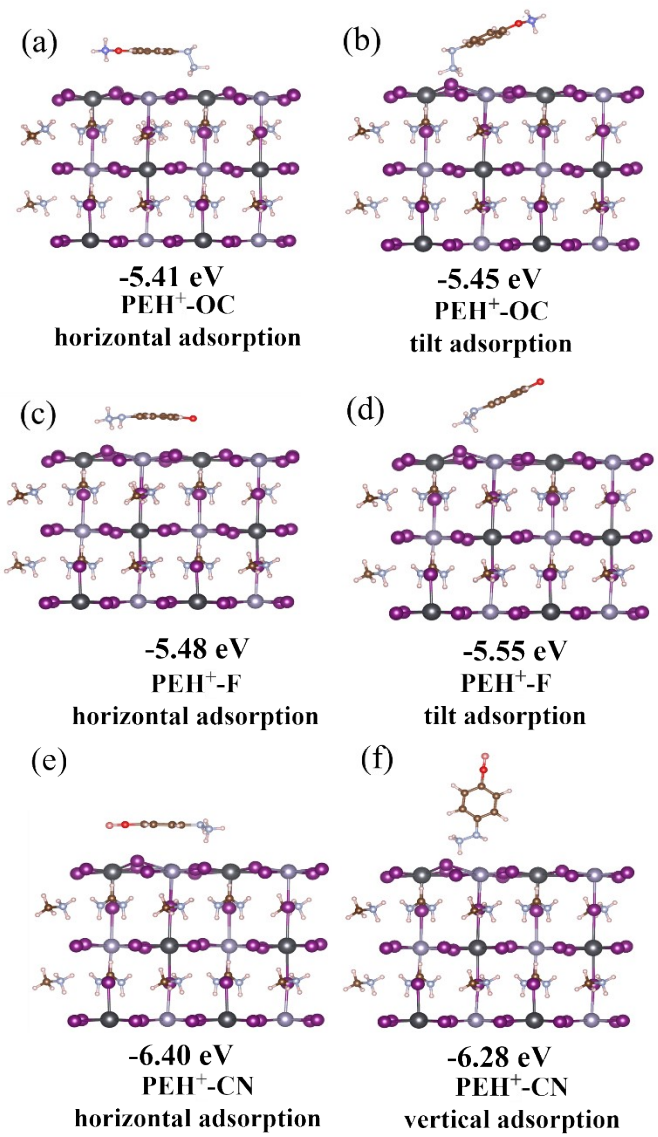

Figure S5. Binding energies of two other possible orientations of PEH^+-X on the Sn-Pb perovskite surface. (a) (b) horizontal and tilted adsorption of PEH^+-OC; (c) (d) horizontal and tilted adsorption of PEH^+-F; (e), (f) horizontal and vertical adsorption of PEH^+-CN.

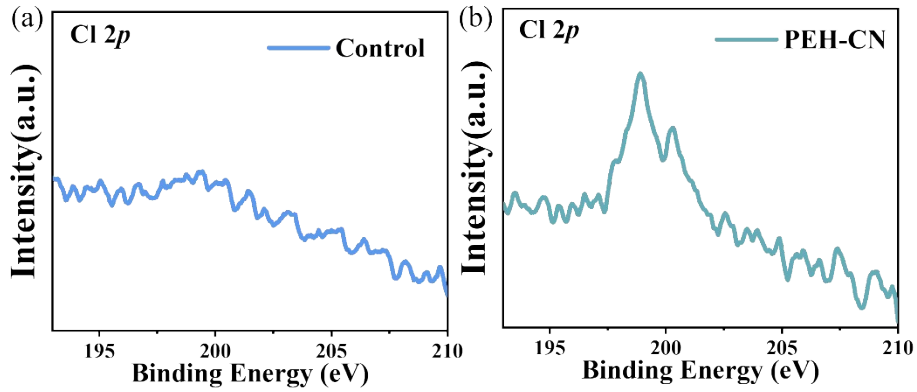

Figure S6. Cl 2*p* XPS spectra of control (a) and PEHCl-CN-modified films (b).

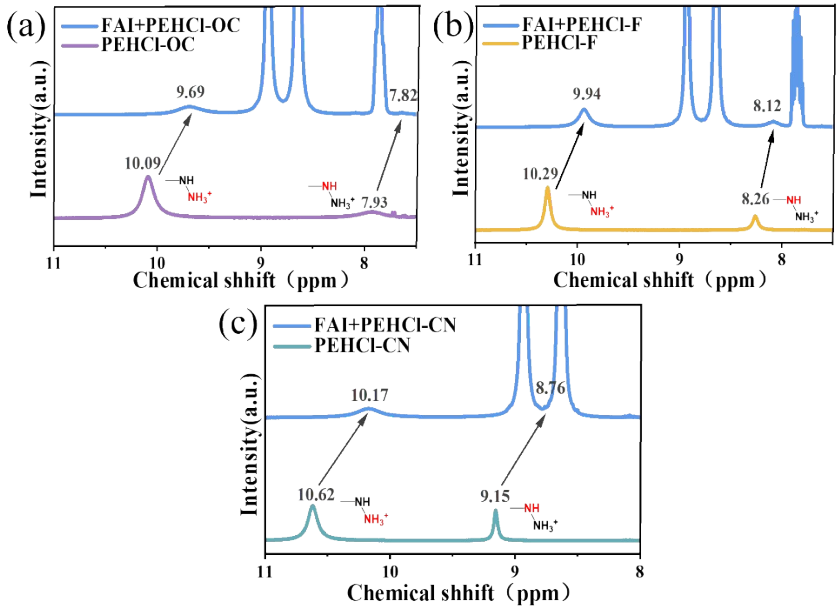

Figure S7. ^{1}H NMR spectra of PEHCl-OC without and with FAI (a), PEHCl-F without and with FAI (b) and PEHCl-CN without and with FAI. The displacement of hydrogen in different chemical environments demonstrates the formation of hydrogen bonds.

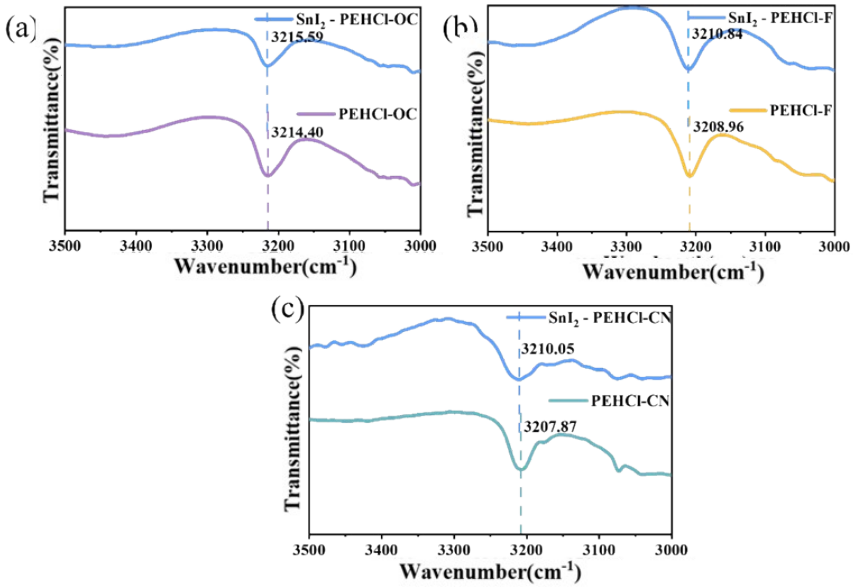

Figure S8. FTIR spectra of PEHCl-OC and SnI_2-PEHCl-OC (a), PEHCl-F and SnI_2-PEHCl-F (b) and PEHCl-CN and SnI_2-PEHCl-CN (c). The displacement of N-H vibrational bonds suggests interaction with SnI_2.

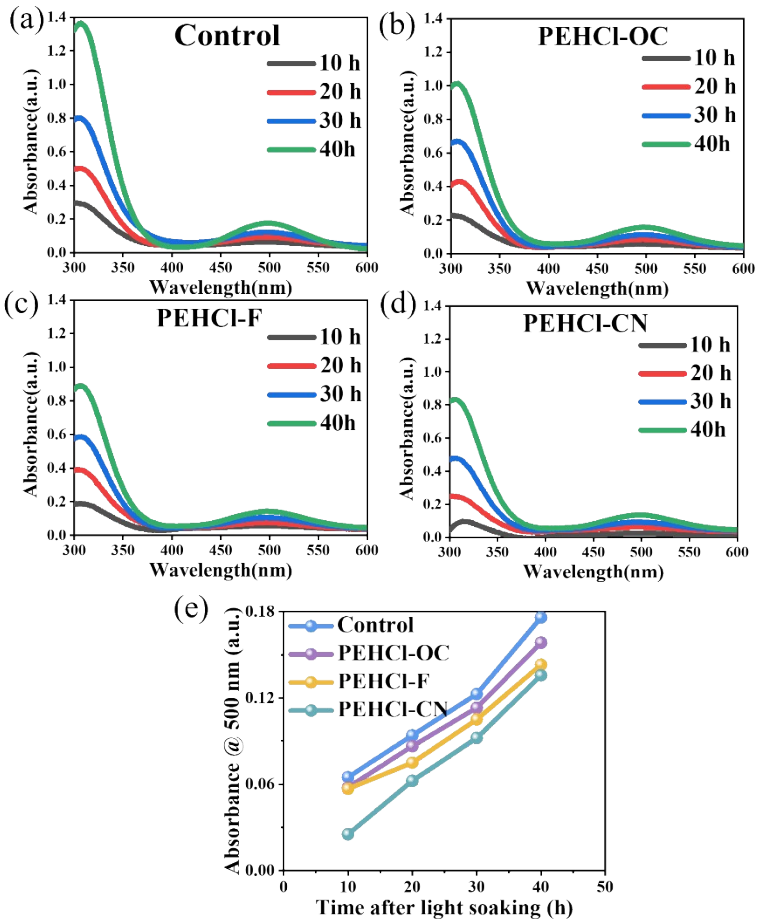

Figure S9. (a), (b), (c), (d) UV absorption spectra of the toluene in which perovskite films of control, PEHCl-OC, PEHCl-F, PEHCl-CN were immersed under 1 sun illumination for 10, 20, 30, and 40 H; (e) The change in absorbance at 500 nm corresponds to the rate of I_2 production. (Since the perovskite film will not dissolve in toluene, the iodine produced will dissolve in toluene, and we can conclude the generation of iodine quantity.)

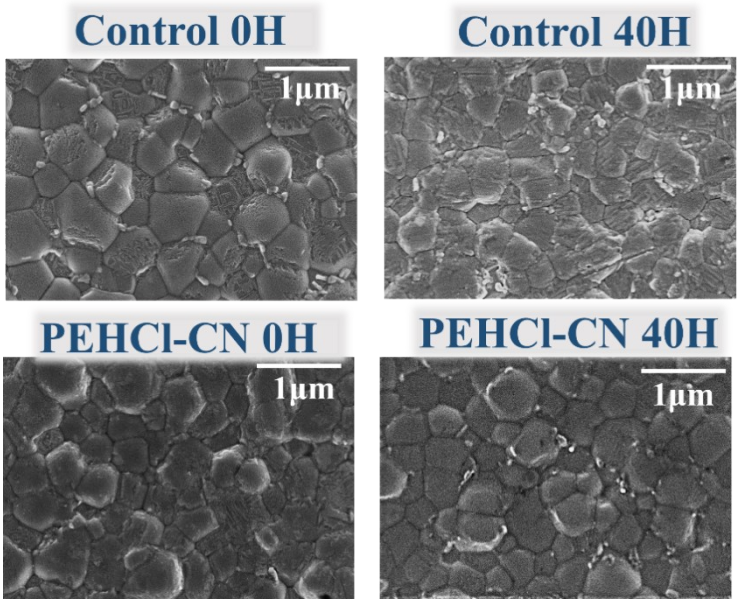

Figure S10. Scanning electron microscopy (SEM) images of the perovskite films under 20 hours and 30 hours. (a, d) pristine perovskite films, and (c, d) perovskite films with PEHCl-CN.

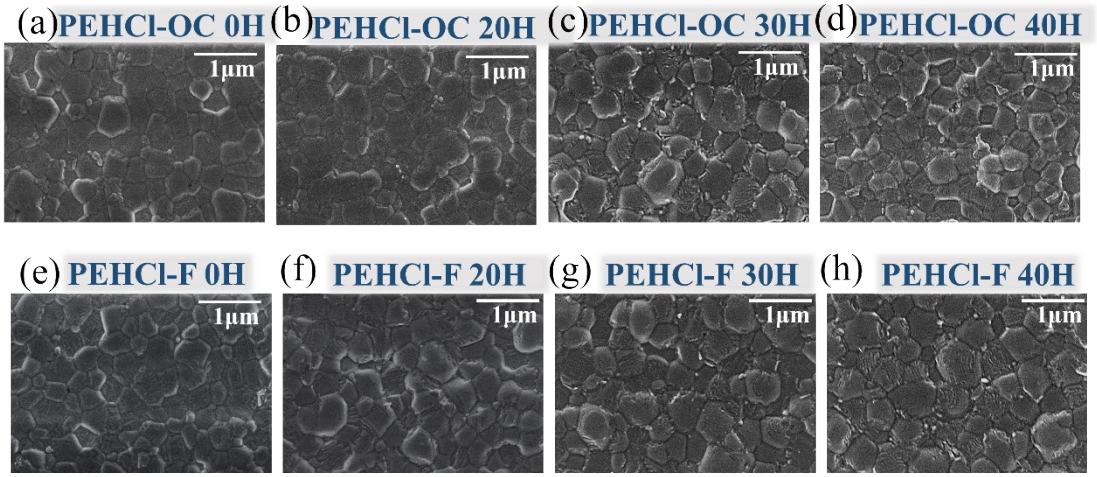

Figure S11. SEM images of the perovskite films under different illumination periods (0 h, 20 h, 30 h, 40 h), (a-d) perovskite films with PEHCl-OC, (e-h) perovskite films with PEHCl-F .

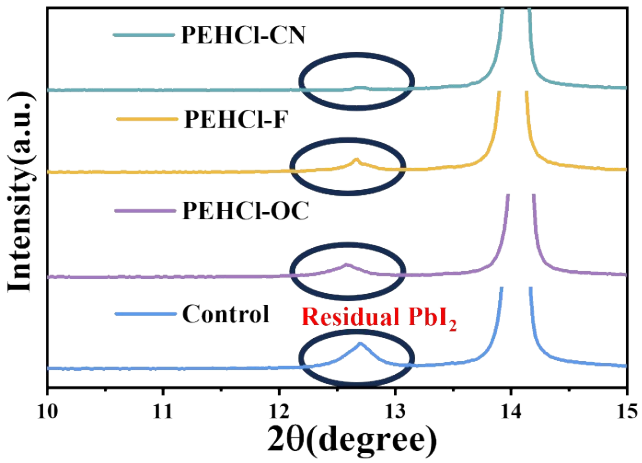

Figure S12. XRD patterns of perovskite films containing an additional 2 mol% PbI_2, without additives and with (PEHCl-X). All additive concentrations are 2 mg/ml.

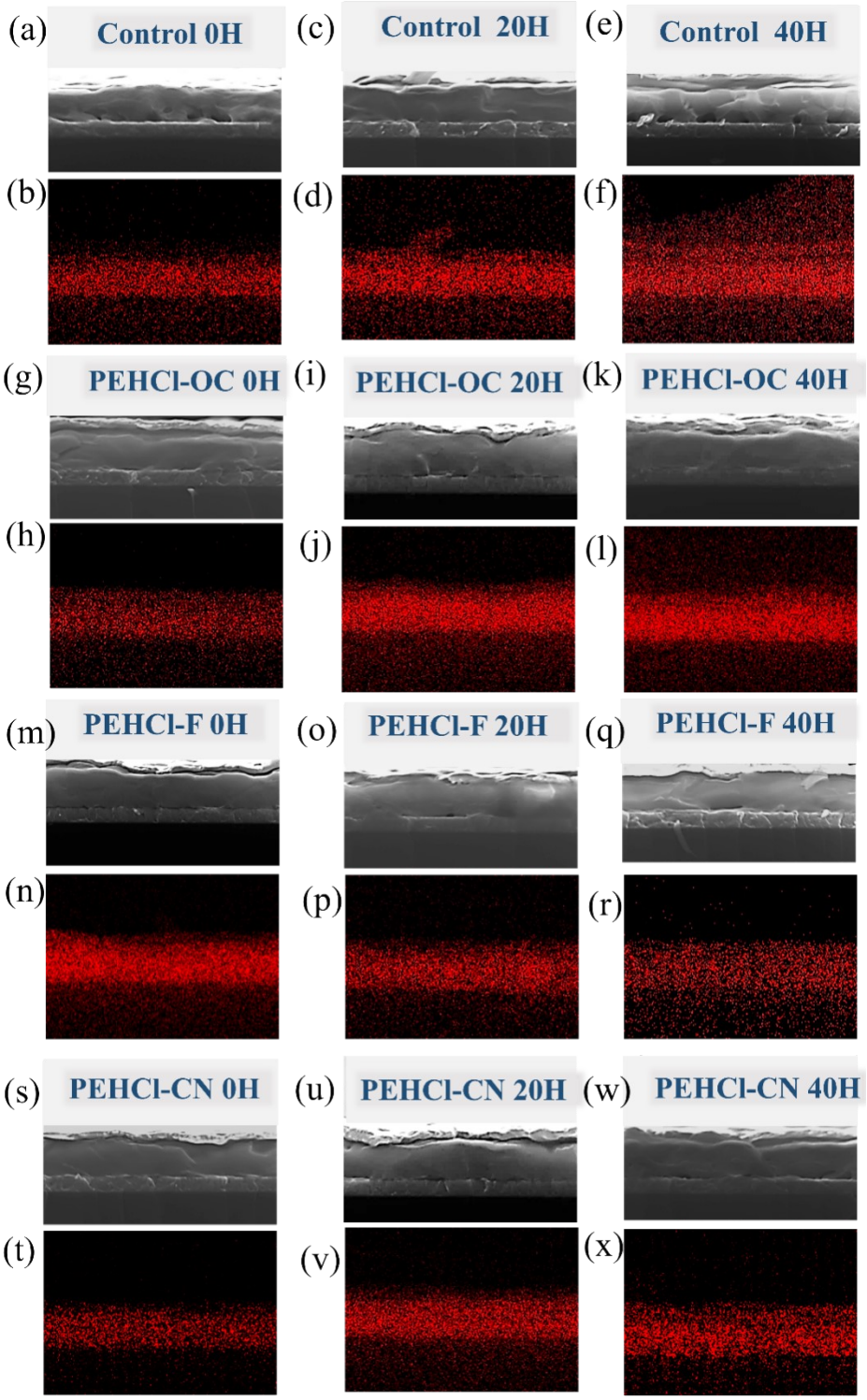

Figure S13. Cross-sectional SEM images and energy dispersive spectroscopy (EDS) of iodide element, (a-f) control, (g-l) with PEHCl-OC, (m-r) with PEHCl-F and (s-x) with PEHCl-CN after different time aging of illumination (20H and 40H). SEM images can evaluate film morphology, and EDS energy spectroscopy can evaluate iodide ion migration.

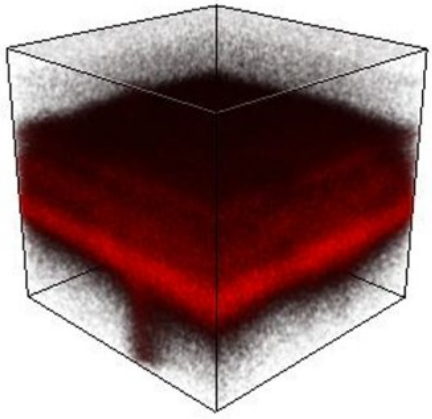

Figure S14. 3D distribution map of Cl^- from ToF-SIMS profiles.

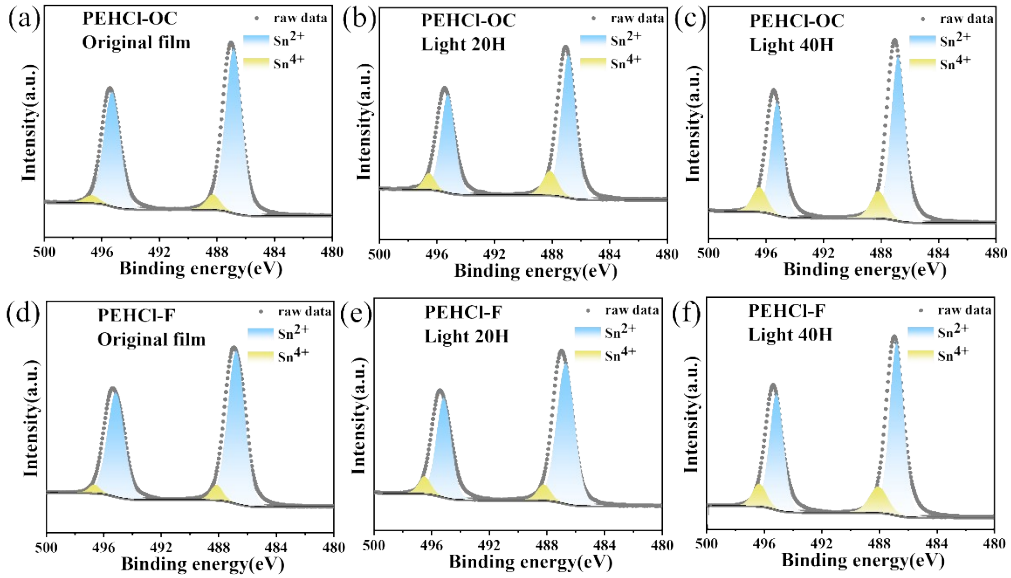

Figure S15. The Sn 3*d* XPS peak images of PEHCl-F treated film (a, b, c) and PEHCl-OC treated film (d, e, f) after aging treatment of 20 and 40 hours of light time.

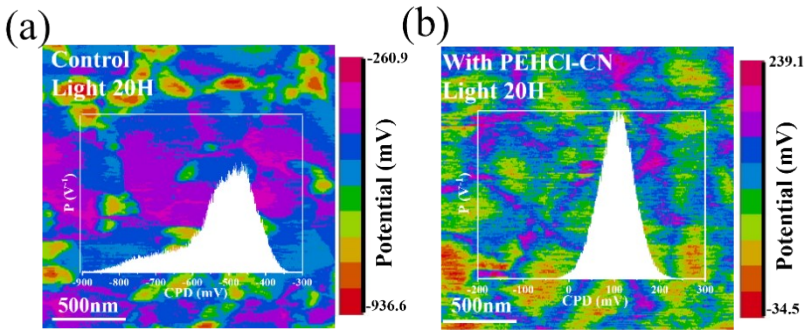

Figure S16. Kelvin probe force microscopy (KPFM) images (with insets of Contact potential difference (CPD) distribution) of control and PEHCl-CN treated films after 20 hours light.

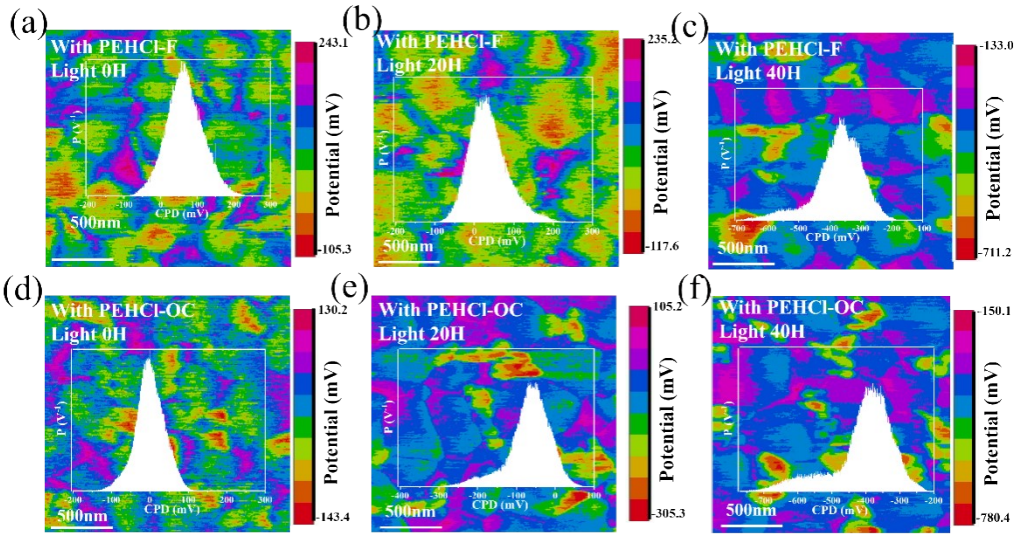

Figure S17. KPFM images of corresponding perovskite films (with insets of Contact potential difference (CPD) distribution) after 0 hour, 20 hours and 40 hours light.

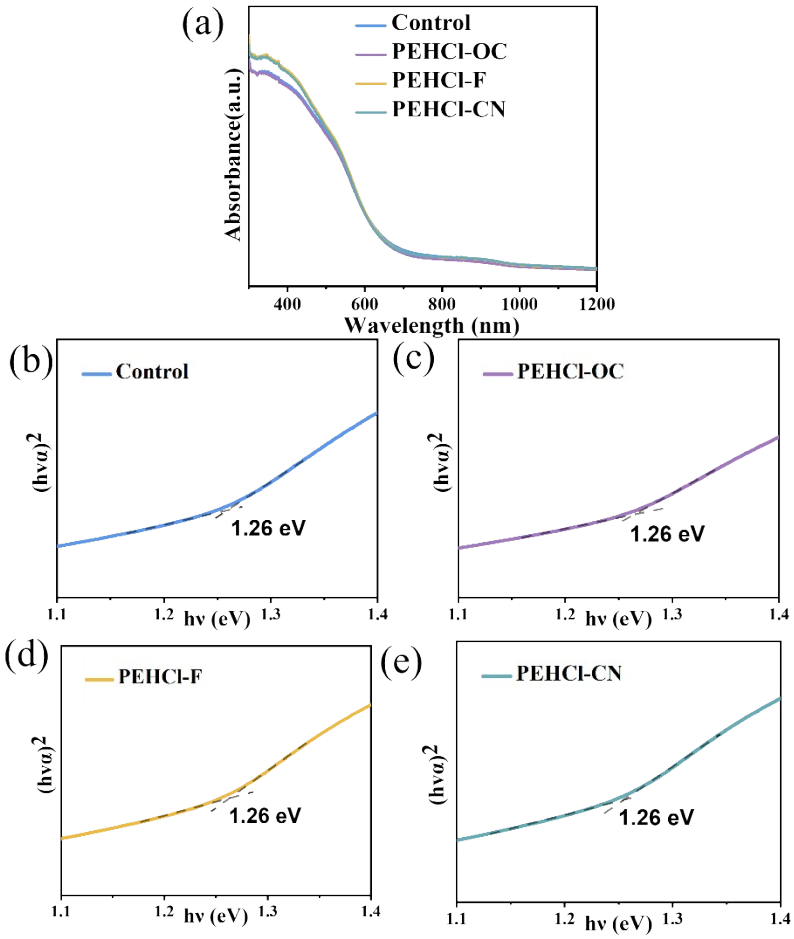

Figure S18. (a) Absorbance spectra and (b-e) Tauc plots of the perovskite films with and without PEH-X processing. The results show that the incorporation of PEHCl-OC, PEHCl-F, and PEHCl-CN (concentration 2 mg/ml) cannot affect the optical band gap of tin-lead perovskite.

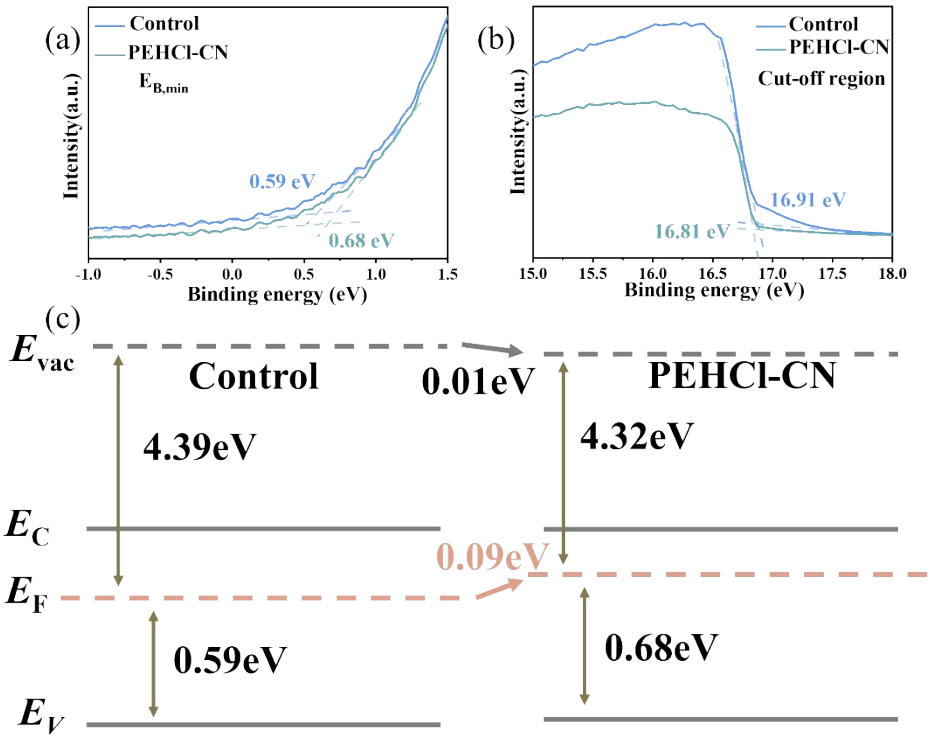

Figure S19. Secondary-electron cut-off energies (a) and onsets of the E_B (b) from UPS spectra of Sn–Pb perovskite films with and without PEHCl-CN processing. (c) Energy level diagram of control (e) and PEHCl-CN-doped perovskite films based on the UPS spectra and Tauc plots (Figure S18).

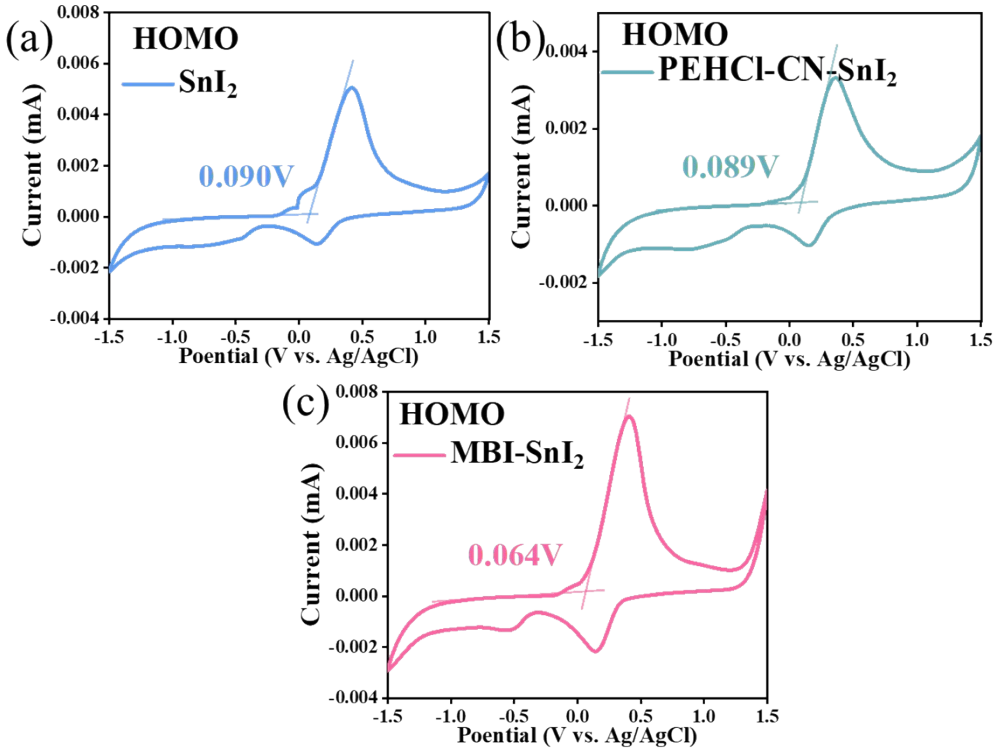

Figure S20. CV curves of the solution (a) SnI_2, (b) SnI_2 with PEHCl-CN and (c) SnI_2 with MBI.

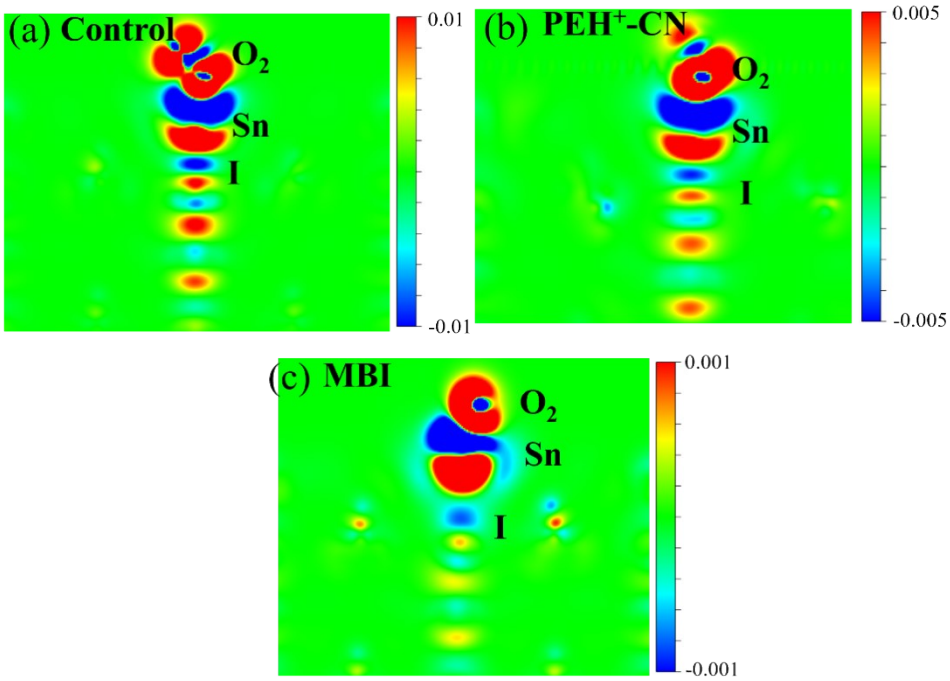

Figure S21. Cross-sectional distribution of charge density of (a) O_2, (b) O_2-PEH^+-CN, and (c) O_2-MBI, after absorption on perovskite. Red represents areas of increased charge, while blue indicates areas of decreased charge. The saturation levels in (a) is 0.01, (b) is 0.005, (c) is 0.001

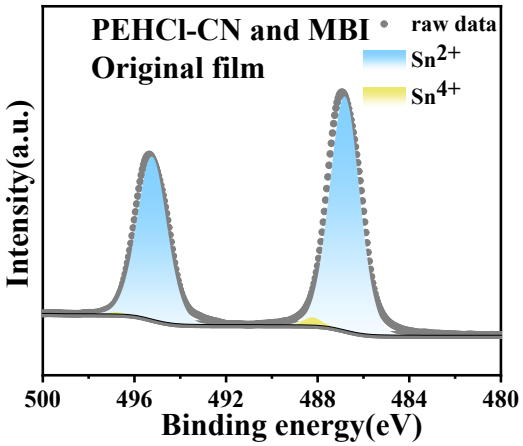

Figure S22. Sn 3*d* XPS peak images of with PEHCl-CN and MBI films.

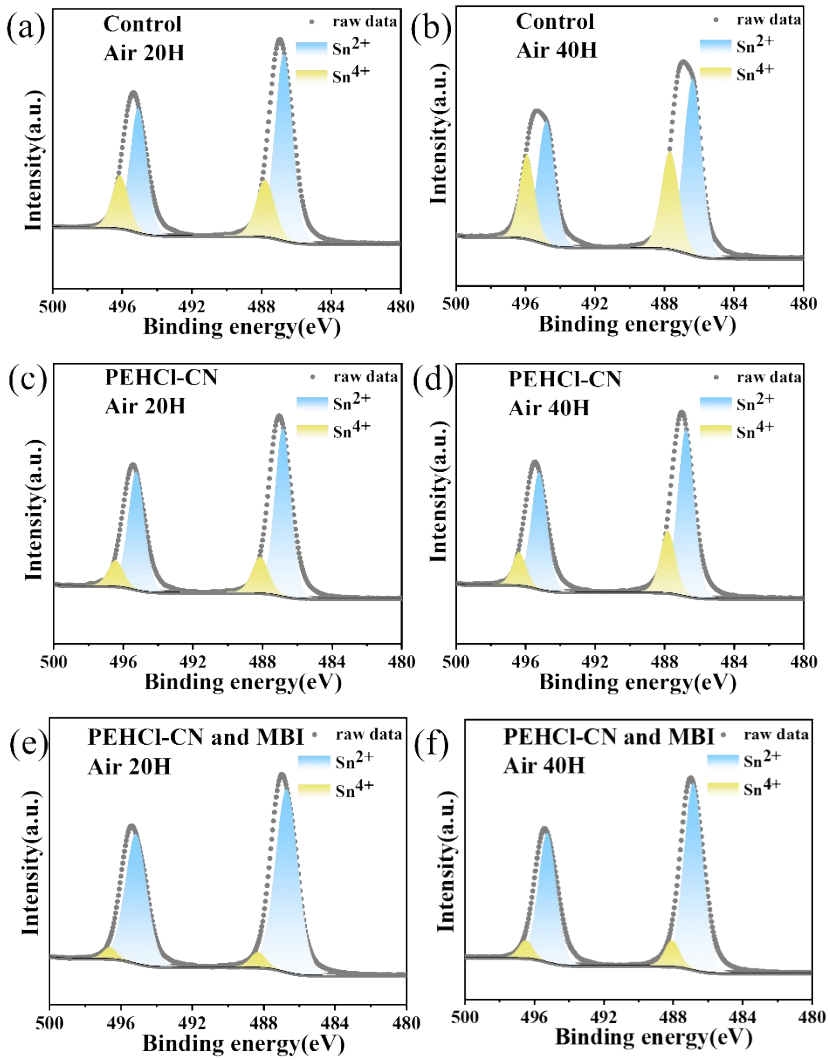

Figure S23. Sn 3*d* XPS peaks of without any treatment films (a, b), with PEHCl-CN treated (c, d) and PEHCl-CN and MBI treated films (e, f) after 20 and 40 hours of air corrosion aging treatment image.

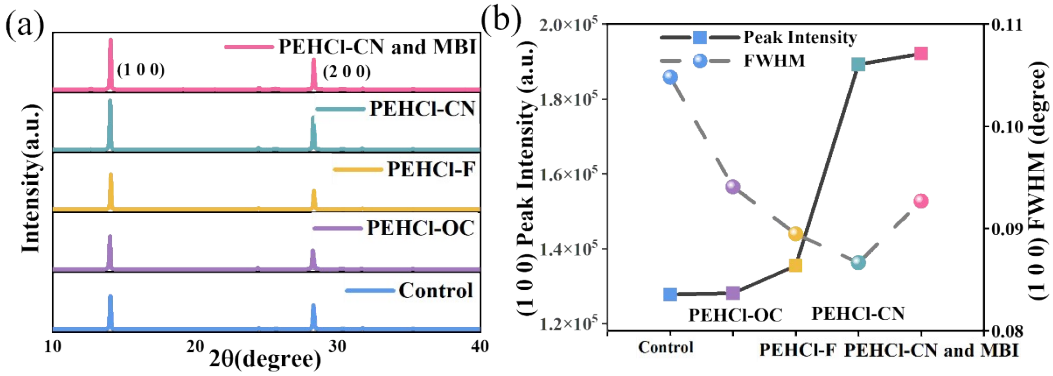

Figure S24. (a) XRD patterns of pristine perovskite film, and with PEHCl-OC, PEHCl-F, PEHCl-CN, PEHCl- CN and MBI perovskite film; (b) the corresponding peak intensity of the (100) peaks and FWHM of (100) peak of the perovskite.

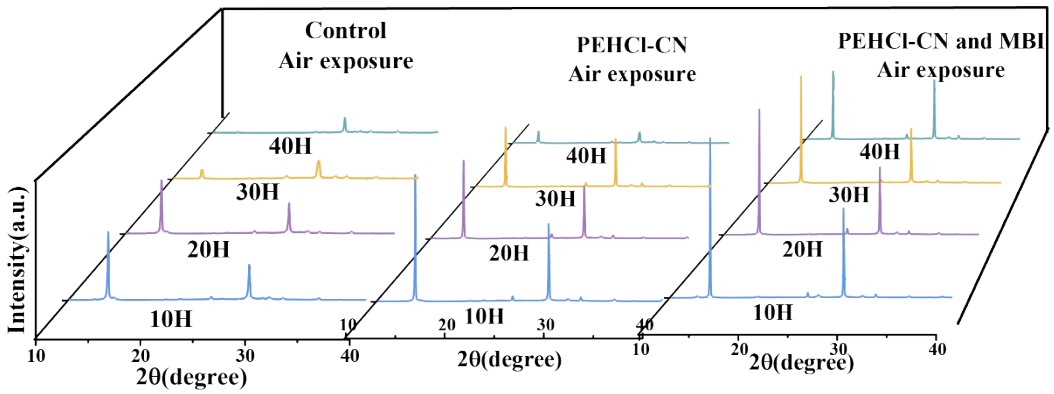

Figure S25. XRD patterns of original, PEH-CN treated and PEH-CN and MBI treated films exposed to air for a series of gradient times (10-40 hours).

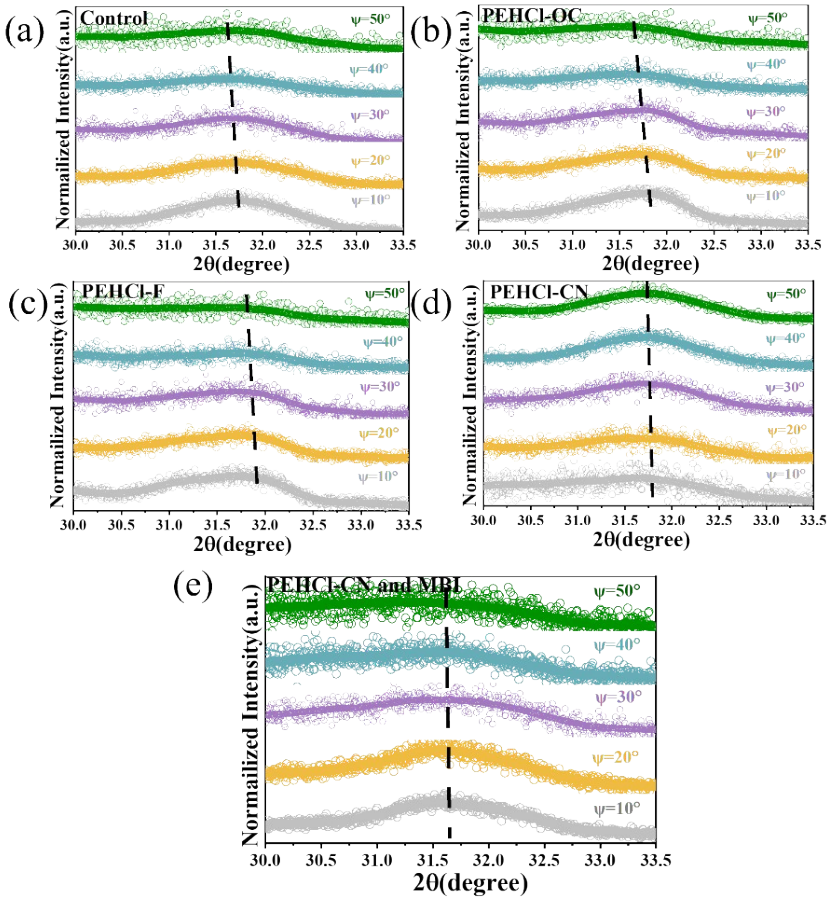

Figure S26. (a) (b) (c) (d) (e) Depth-resolved grazing incident XRD (GIXRD) spectra at different Ψ angles (from 10°to 50°) of five films.

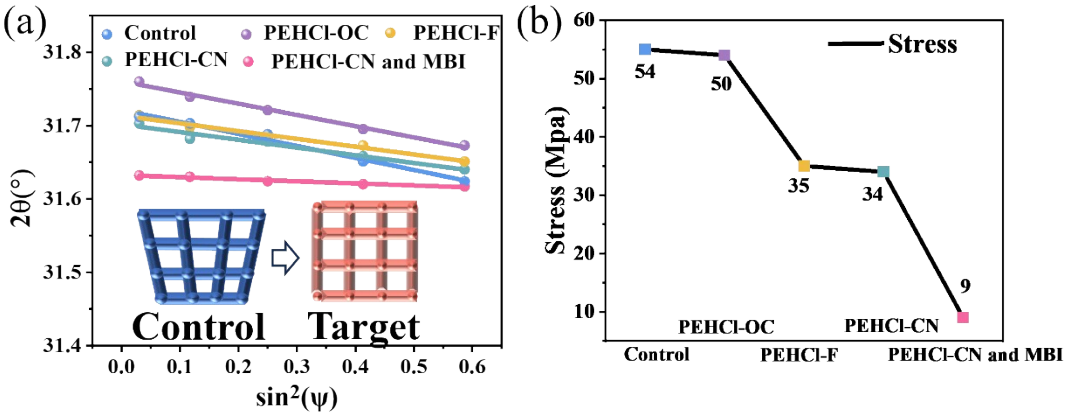

Figure S27. (a) Linear fit of 2θ-sin^2 (Ψ) for perovskite films derived from GIXRD (the inset is an illustration of the relaxation of tensile strains); (b) the tensile strain statistical magnitudes of five films.

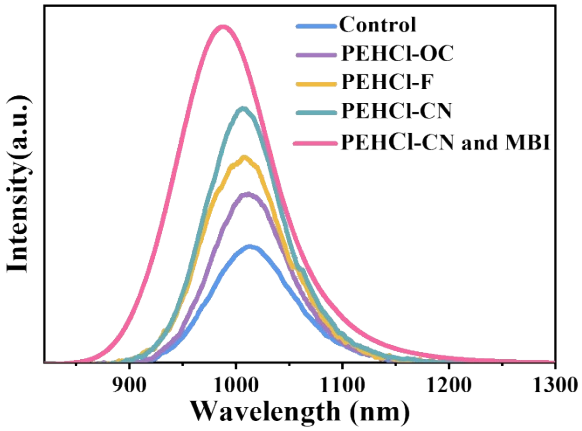

Figure S28. Steady-state photoluminescence (PL) spectra.

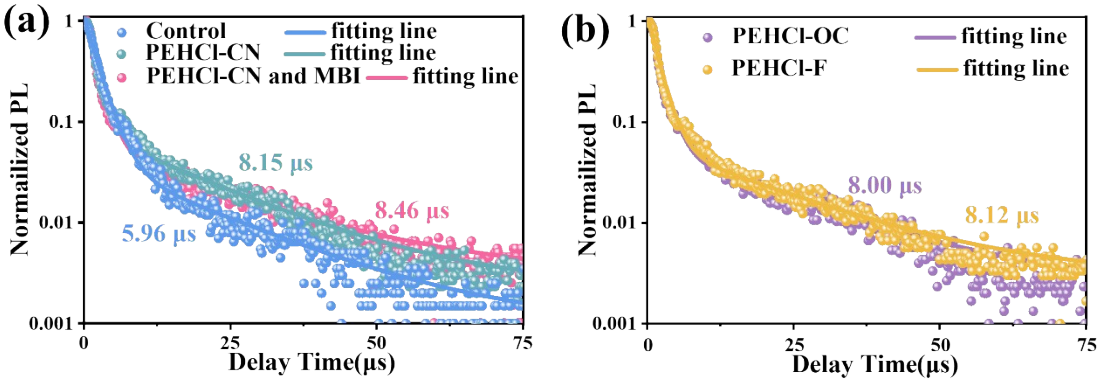

Figure S29. Time-resolved photoluminescence (TRPL) decay curves of the control, PEHCl-CN-treated , PEHCl-CN and MBI-treated (a), Sn-Pb perovskite films; the PEH-OC-treated , PEHCl-F-treated (b) are shown in (b).

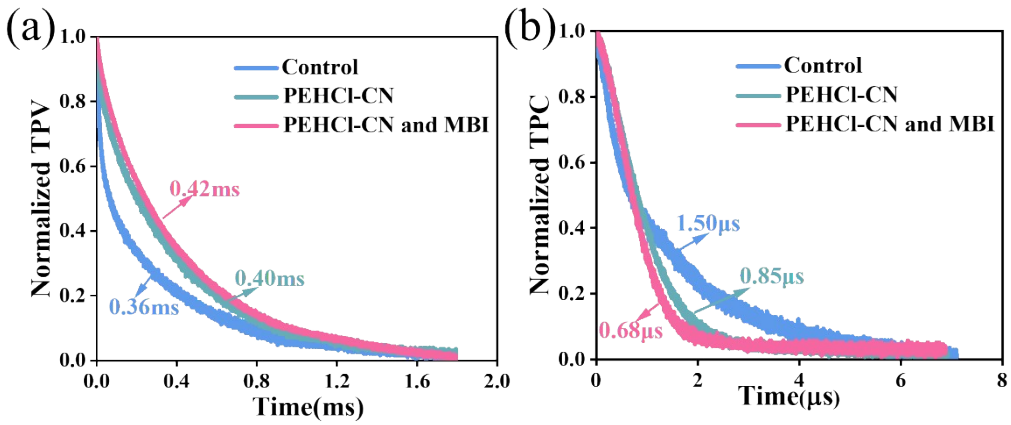

Figure S30. Transient photovoltage (TPV) decay curves (a); Transient photocurrent (TPC) decay curves.

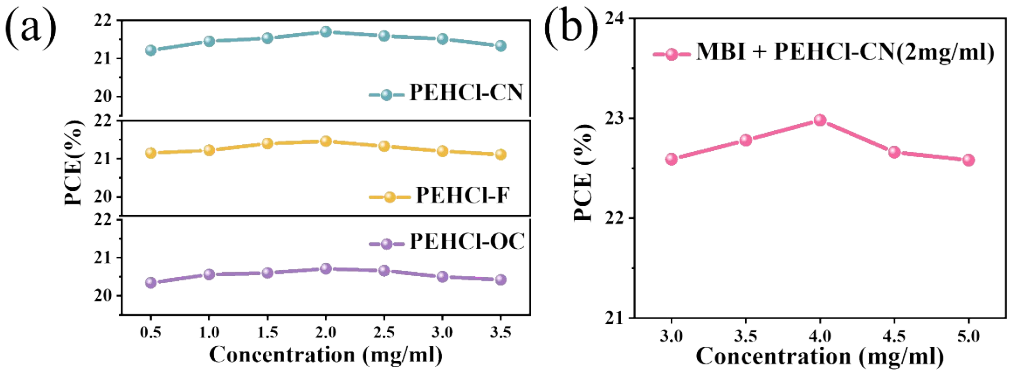

Figure S31. PCE trend of additives with varying concentration.

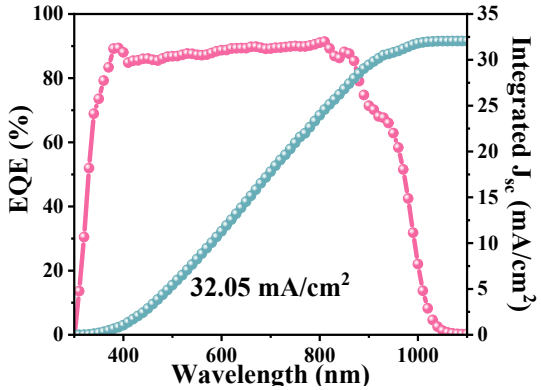

Figure S32. EQE spectra of single-junction Sn-Pb cell.

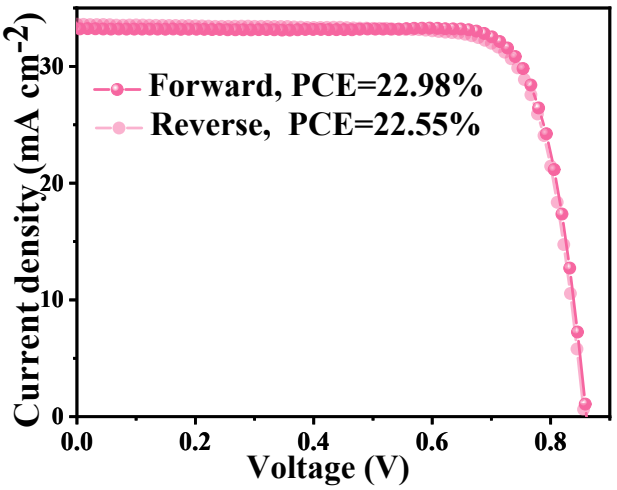

Figure S33. Forward scanned and reverse scanned J-V curves of PEHCl-CN and MBI-treated PSC.

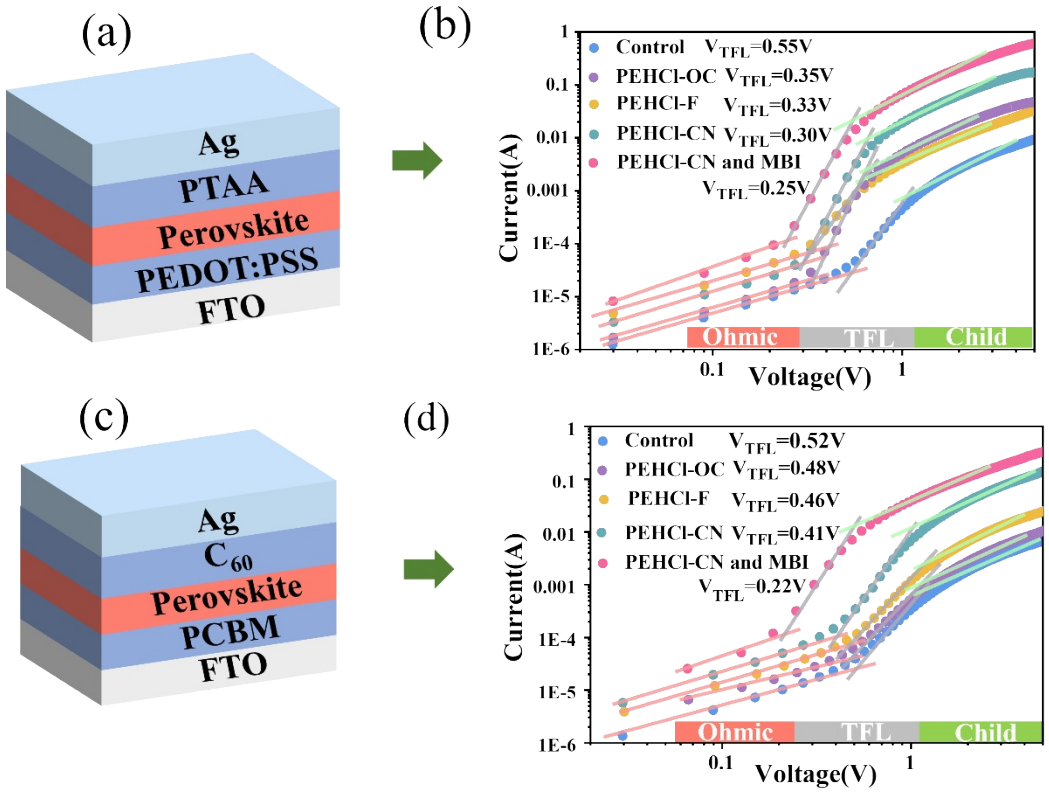

Figure S34. Space-charge-limited current (SCLC) analysis of hole-only devices and electron -only devices. Device structure (a, c) and fitting results (b, d).

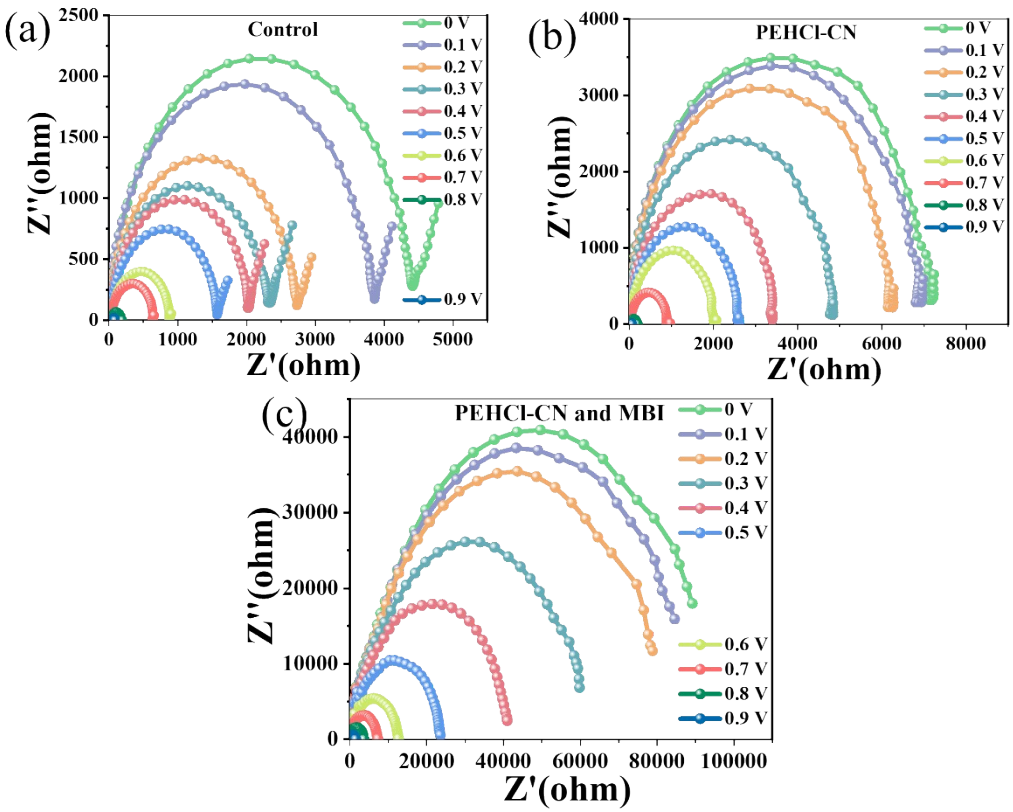

Figure S35. Nyquist plots of PSC devices based on (a) pristine perovskite film, (b) PEHCl-CN-treated perovskite film, (c) PEHCl-CN and MBI-treated perovskite film at different bias (from 0 V to 0.9 V).

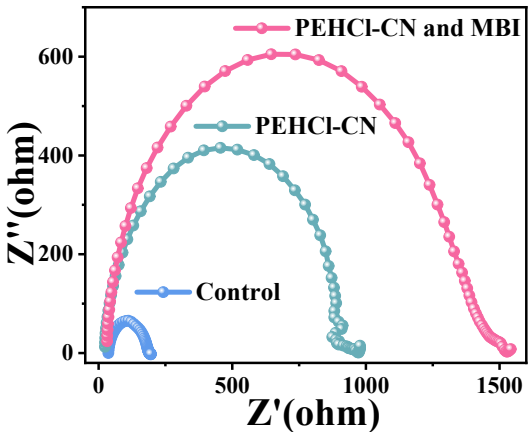

Figure S36. Nyquist plots of PSCs at 0.4 V with a frequency range between 1MHz and 1 Hz.

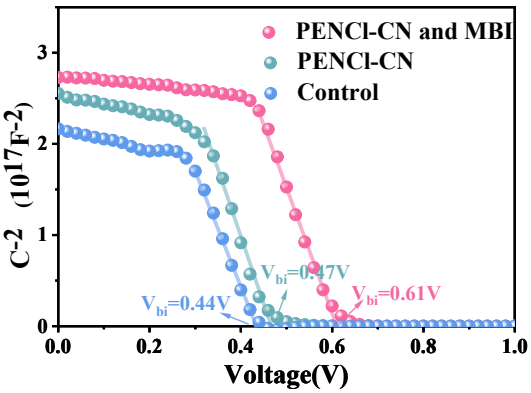

Figure S37. Mott-Schottky plots of the control, PEHCl-CN treated and PEHCl-CN and MBI treated devices.

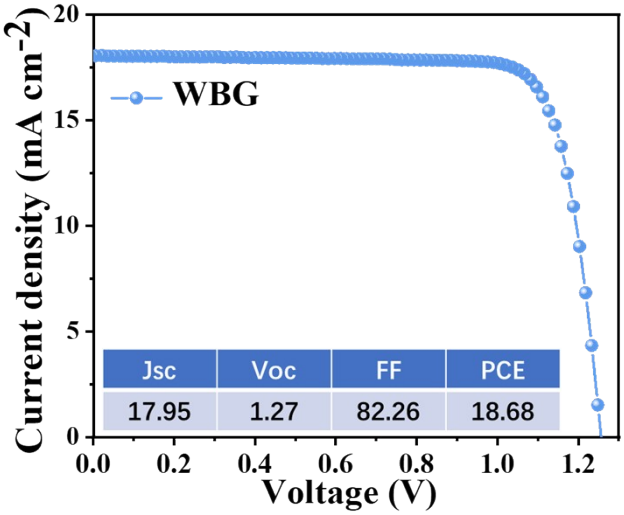

Figure S38. J-V curve of wide bandgap cell and its parameters.

Test and Calibration Center of New Energy Device and Module,
Shanghai Institute of Microsystem and Information Technology,
Chinese Academy of Sciences (SIMIT)

Measurement Report

Report No. 24TR040101

Client Name	Ningbo Institute of Materials Technology and Engineering (NIMTE), Chinese Academy of Sciences (CAS)
Client Address	1219 Zhongguan West Road, Ningbo, China (315201)
Sample	Perovksite/perovskite tandem solar cell
Manufacturer	Ningbo Institute of Materials Technology and Engineering (NIMTE), Chinese Academy of Sciences (CAS)
Measurement Date	1st April, 2024

Performed by:	Qiang Shi	**Date:** 01/04/2024
Reviewed by:	Wenjie Zhao	**Date:** 01/04/2024
Approved by:	Yucheng Liu	**Date:** 01/04/2024

Address: No.235 Chengbei Road, Jiading, Shanghai **Post Code:**201800
E-mail: solarcell@mail.sim.ac.cn **Tel:** +86-021-69976905

Sample Information

Sample Type	Perovskite/perovskite tandem solar cell
Serial No.	1-1
Lab Internal No.	24040101-1#
Measurement Item	I-V characteristic
Measurement Environment	24.3±2.0°C, 42.3±5.0%R.H

Measurement of I-V characteristic

Reference cell	PVM1121
Reference cell Type	mono-Si, WPVS, calibrated by NREL (Certificate No. ISO 2098)
Calibration Value/Date of Calibration for Reference cell	143.95mA/ Feb. 2024
Measurement Conditions	Standard Test Condition (STC): Spectral Distribution: AM1.5 according to IEC 60904-3 Ed.3, Irradiance: 1000±50W/m^2, Temperature: 25±2°C
Measurement Equipment/ Date of Calibration	AAA Steady State Solar Simulator (YSS-T155-2M) / July.2023 IV test system (ADCMT 6246) / June. 2023 Measuring Microscope (MF-B2017C) / July.2023 SR Measurement system (CEP-25ML-CAS) / April.2023
Measurement Method	I-V Measurement: Logarithmic sweep in reverse direction (Voc to Isc) during one flash based on IEC 60904-1:2020; Spectral Mismatch factor was calculated according to IEC 60904-7 and I-V correction according to IEC 60891.
Measurement Uncertainty	Area: 1.1%(k=2); Isc: 2.4%(k=2); Voc: 1.0%(k=2); Pmax: 2.8%(k=2); Eff: 3.0%(k=2)

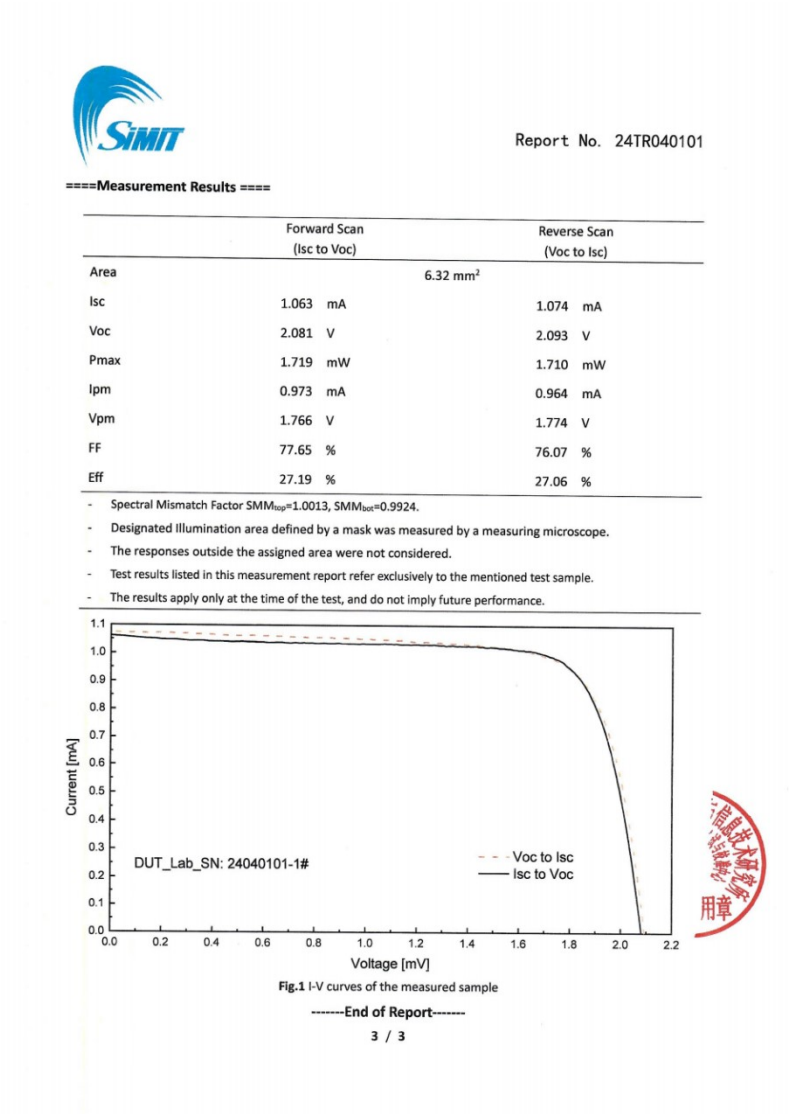

Report No. 24TR040101

====Measurement Results ====

	Forward Scan (Isc to Voc)	Reverse Scan (Voc to Isc)
Area	6.32 mm²	
Isc	1.063 mA	1.074 mA
Voc	2.081 V	2.093 V
Pmax	1.719 mW	1.710 mW
Ipm	0.973 mA	0.964 mA
Vpm	1.766 V	1.774 V
FF	77.65 %	76.07 %
Eff	27.19 %	27.06 %

- Spectral Mismatch Factor SMM_{top}=1.0013, SMM_{bot}=0.9924.
- Designated Illumination area defined by a mask was measured by a measuring microscope.
- The responses outside the assigned area were not considered.
- Test results listed in this measurement report refer exclusively to the mentioned test sample.
- The results apply only at the time of the test, and do not imply future performance.

Fig.1 I-V curves of the measured sample

-------End of Report-------

3 / 3

Figure S39. Certification report for a representative all-perovskite tandem cell based on a PEHCl-CN and MBI-modified Sn-Pb sub-cell by Shanghai Institute of Microsystem and Information Technology (SIMIT).

The content of Sn^{4+}(%)	Original film	Light 20H	Light 40H	Air 20H	Air 40H
Control	12.66	18.59	24.97	26.29	36.58
PEHCl-OC	6.01	13.29	16.64	\	\
PEHCl-F	5.54	9.16	15.89	\	\
PEHCl-CN	4.98	6.38	7.86	17.52	23.42
PEHCl-CN and MBI	1.31	\	\	5.08	9.49

Table S1. Specific percentages of all XPS peaks (Sn^{4+}) under different conditions.

	τ_1	τ_2	τ_{ave}
Control	2.15E+03	1.77E+04	5.96E+03
PEHCl-OC	1.73E+03	1.95E+04	8.00E+03
PEHCl-F	1.76E+03	1.93E+04	8.12E+03
PEHCl-CN	1.81E+03	1.72E+04	8.15E+03
PEHCl-CN and MBI	1.77E+03	2.06E+04	8.46E+03

Table S2. Fitting parameters of TRPL for control and target perovskite films.

H-ONLY	V_{TFL} (V)	N_t (cm^{-3})
Control	0.55	8.51058E+16
PEHCl-OC	0.35	5.41582E+16
PEH-F	0.33	5.10635E+16
PEHCl-CN	0.30	4.64213E+16
PEHCl-CN and MBI	0.25	3.86844E+16

Table S3. Results derived from hole-only SCLC.

E-ONLY	V_{TFL} (V)	N_t (cm^{-3})
Control	0.52	8.04636E+16
PEHCl-OC	0.48	7.42741E+16
PEHCl-F	0.46	7.11794E+16
PEHCl-CN	0.41	6.34425E+16
PEHCl-CN and MBI	0.22	3.40423E+16

Table S4. Results derived from electron-only SCLC.

NBG	J_{sc}	V_{oc}	*FF*	*PCE(%)*
Control	31.66	0.83	75.35	20.1
PEHCl-OC	31.49	0.86	76.41	20.7
PEHCl-F	32.99	0.86	76.01	21.4
PEHCl-CN	32.87	0.85	78.1	21.7
PEHCl-CN and MBI	33.23	0.86	80.34	23.0

Table S5. Parameters of the single-junction Sn-Pb solar cells.

Tandem	J_{sc}	V_{oc}	*FF*	*PCE(%)*
Control	15.89	2.04	78.1	25.4
PEHCl-CN and MBI	16.48	2.08	81.4	27.9
PEHCl-CN and MBI certified device	16.82	2.08	77.7	27.2

Table S6. Parameters of the tandem solar cells.